Ecotoxicology and Environmental Safety 147 (2018) 919–925

Contents lists available at ScienceDirect

Ecotoxicology and Environmental Safety

journal homepage: www.elsevier.com/locate/ecoenv

Response surface methodology modeling to improve degradation of Chlorpyrifos in agriculture runoff using TiO_2 solar photocatalytic in a raceway pond reactor

Hoda Amiri[a], Ramin Nabizadeh[a,b], Susana Silva Martinez[c], Seyed Jamaleddin Shahtaheri[d], Kamyar Yaghmaeian[a,e], Alireza Badiei[f], Shahrokh Nazmara[a,e], Kazem Naddafi[a,b,*]

[a] Department of Environmental Health Engineering, School of Public Health, Tehran University of Medical Sciences, Tehran, Iran
[b] Center for Air Pollution Research (CAPR), Institute for Environmental Research (IER), Tehran University of Medical Sciences, Tehran, Iran
[c] Centro de Investigación en Ingeniería y Ciencias Aplicadas, Av. Universidad 1001, Col. Chamilpa, Cuernavaca, Morelos, Mexico
[d] Department of Occupational Health Engineering, School of Public Health, Institute for Environmental Research, Tehran University of Medical Sciences, Tehran, Iran
[e] Center for Water Quality Research (CWQR), Institute for Environmental Research (IER), Tehran University of Medical Sciences, Tehran, Iran
[f] School of Chemistry, College of Science, University of Tehran, Tehran, Iran

ARTICLE INFO

Keywords:
Chlorpyrifos
TiO_2 catalyst
POPs
RPR
Solar
RSM

ABSTRACT

This paper deals with the use of a raceway pond reactor (RPR) as an alternative photoreactor for solar photocatalytic applications. Raceway pond reactors are common low-cost reactors which can treat large volumes of water. The experiments were carried out with TiO_2 in the agriculture effluent spiked with Chlorpyrifos (CPF) at circumneutral pH. The Response Surface Methodology (RSM) was used to find the optimum process parameters to maximize CPF oxidation from the mathematical model equations developed in this study using R software. By ANOVA, p-value of lack of fit > 0.05 indicated that, the equation was well-fitted. The theoretical efficiency of CPF removal, under the optimum oxidation conditions with UV solar energy of around 697 ± 5.33 lux, was 84.01%, which is in close agreement with the mean experimental value (80 ± 1.42%) confirming that the response model was suitable for the optimization. As far as the authors know, this is the first study of CPF removal using RPR in agriculture runoff at circumneutral pH.

1. Introduction

Organophosphorus insecticides such as Chlorpyrifos are the most widely used pesticides in the world. Chlorpyrifos, a broad spectrum non-systemic organophosphate insecticide used to control many different insects, is highly toxic to non-target organisms, including mankind (Ejaz et al., 2017).

According to the Stockholm Convention, Chlorpyrifos (alternative to endosulfan) is a substance considered by the Persistent Organic Pollutants Review Committee (POPRC) to meet the POP criteria but remained undetermined due to misleading or insufficient data (UNEP, 2012). In addition, the EPA has reviewed the human health risk assessment and assessment of potable water exposure for Chlorpyrifos in 2015. The revised analysis showed the risks of dietary exposure (ie residues of Chlorpyrifos in food crops) and potable water (EPA, 2015). Chlorpyrifos has a relatively low water solubility (2.0 mg L^{-1} at 25 °C), while its octanol water partitioning is high (log K_{ow} = 4.7 at 20 °C) which tend to concentrate on lipid portion of the membrane (WHO, 2009). The greatest use of Chlorpyrifos is in cotton, rice, corn, tobacco, almonds, beans, maize and fruit trees including oranges, bananas, apples and vegetables. It has been marked in the blood of umbilical cord, the human breast milk, the cervical fluid, the sperm fluid, and the meconium of new born infants. The health problem of Chlorpyrifos includes miosis, increased urination, diarrhea, diaphoresis, tearing and salivation. Accommodates in the human body and Fauna by contact with the skin, ingestion and vapor action (Sharbidre et al., 2011). Because of these causes of health effects, it is necessary to use alternative technologies such as advanced oxidation processes (AOP) to remove pesticides from water. AOP represent excellent processes of elimination of organic pollutants in water, because the hydroxyl radicals ($HO^{\bullet}$) produced during these processes are capable of non-selectively enhancing both degradation and mineralization of the pollutants in CO_2, H_2O and inorganic salts (Zimbron and Reardon, 2009). Among the latest technologies, photocatalysis is one of the most advanced and developed technologies to eliminate pollutants from the environment. Titanium dioxide (TiO_2), due to its strong oxidizing power and long-term

* Corresponding author at: Department of Environmental Health Engineering, School of Public Health, Tehran University of Medical Sciences, Tehran, Iran.
E-mail address: knadafi@tums.ac.ir (K. Naddafi).

http://dx.doi.org/10.1016/j.ecoenv.2017.09.062
Received 9 August 2017; Received in revised form 19 September 2017; Accepted 22 September 2017

photochemical resistance to corrosion, is an efficient semiconductor well known for its extensive application in the degradation of different contaminants in both gaseous and liquid phases (Khan et al., 2008). TiO_2 photocatalyst has been used mainly in environmental remediation (ie, detoxification of wastewater) and conversion of solar energy (Fujishima and Zhang, 2006; Wang et al., 2006). TiO_2 (band gap energy 3.2 eV) upon illumination with UV light ($\lambda < 380$ nm) produces excited high-energy states of electron (in the conduction band, e^-_{cb}) and hole (in the valence band, h^+_{vb}) pairs, reaction (1), capable of initiating chemical reactions (Gaya and Abdullah, 2008).

$$TiO_2 + hv \rightarrow e^-_{cb} + h^+_{vb} \quad (1)$$

The holes are responsible for the degradation of organic compounds and can react with water (reactions 2) or hydroxyl ions (reaction 3) to produce hydroxyl radicals; though, the recombination of the e^-_{cb}/h^+_{vb} pair (reaction 4) and the reduction of $^{\bullet}OH$ radicals (reaction 5) produce large inefficiencies in the photocatalytic process (Choi et al., 1994).

$$H_2O + h^+_{vb} \rightarrow {}^{\bullet}OH + H^+ \quad (2)$$

$$OH^- + h^+_{vb} \rightarrow {}^{\bullet}OH \quad (3)$$

$$h^+_{vb} + e^-_{cb} \rightarrow TiO_2 + \text{heat} \quad (4)$$

$$^{\bullet}OH + e^-_{cb} \rightarrow OH^- \quad (5)$$

The oxidation of organic pollutants (R-H) can take place by a direct reaction with holes (reaction 6) or indirectly via hydroxyl radicals (reaction 7) or free organic radicals (reaction 8) (Fujishima et al., 2000; Gaya and Abdullah, 2008):

$$R - H + h^+_{vb} \rightarrow R^{+\bullet} + \overset{\text{Degradation products}}{} \quad (6)$$

$$R - H + OH^{\bullet} \rightarrow R^{\bullet} + H_2O \quad (7)$$

$$R^{\bullet} + O_2 \rightarrow RO_2^{\bullet} \rightarrow CO_2 + \text{intermediates} \quad (8)$$

The hydroxyl radicals, generated under ambient conditions in these processes, are non-selective powerful oxidant species capable of converting organic pollutants (toxic and non-biodegradable) into relatively innocuous end products such as CO_2, H_2O and mineral acids (Hoffmann et al., 1995).

Although, several studies have used AOP for the degradation of various pollutants including pesticides, Chlorpyrifos (Affam and Chaudhuri, 2013; Amalraj and Pius, 2015; Saini and Kumar, 2016; Sivagami et al., 2016) and organic pollutants, the economic possibility of this approach is often not acceptable. In addition, it is necessary to evaluate essential data on the degradation and formation of reaction byproducts (Hoseini et al., 2013b; Ismail et al., 2013). As for the first factor, the most popular photoreactors are compound parabolic collectors (CPCs), developed for these applications at the end of the nineties. The cost of installing and purchasing a large-scale CPC plant for solar reactions, reaction time, long process times, increase the required solar collector surface and energy consumption for pumping, increasing the costs of installation, operation and maintenance of the process. A better choice reactor would be an extensive and non-concentrating reactor, such as the Raceway Pond Reactor (RPR). In the RPR the liquid depth can be varied and the flow is controlled. It is wide reactor with channels through which the water is recirculated. Powerful, extensive and low-cost RPR photoreactors would spread the use of the photo-Fenton process as tertiary treatment (Carra et al., 2014).

RSM is a collection of mathematical and statistical techniques for the construction of experimental models, in which, two steps are necessary, the definition of an approximation function and the design of the experimental plan. The purpose of RSM application is to minimize the cost of costly analytical methods and associated numerical noise (Bezerra et al., 2008; Dehghani et al., 2017).

In light of these facts, this work aims to investigate the potential of TiO_2 photocatalysis under visible light (artificial solar radiation) for the degradation of Chlorpyrifos in agriculture runoff under real conditions. For this, a lab scale RPR with TiO_2 artificial solar photocatalysis was designed as alternative treatment technology. Since the pH of the solution affects the formation of hydroxyl radicals, by the reaction between hydroxide ions and photoinduced holes on the surface of TiO_2, positive holes are well thought of as the main oxidation steps at low pH; while hydroxyl radicals were considered as the main species at neutral or high pH levels. This may cause higher generation of OH^- due to the presence of more available hydroxyl ions on the TiO_2 surface. Therefore, the degradation efficiency of the process will be logically enhanced at high and natural pH (Ahmed et al., 2011). The experiments were carried out with TiO_2 in the agriculture effluent spiked with Chlorpyrifos (CPF) at circumneutral pH (6.8 ± 0.3).

2. Experimental

2.1. Standards and reagents

The analytical standard of Chlorpyrifos was purchased from Dr Ehrenstorfer (Germany, > 99%purity). TiO_2 Aeroxide P25 (21 nm primary particle size (TEM), ≥99.5% trace metals basis) was provided by Sigma-Aldrich. Acetonitrile (chromatography grade) was purchased from Merck (Darmstadt, Germany). Chlorpyrifos stock solutions (1000 mg L^{-1}) were prepared by dissolving solid Chlorpyrifos in acetonitrile. Various concentrations of Chlorpyrifos solutions (1–4 mg L^{-1}) were spiked in the agriculture effluent from stock solution.

2.2. Experimental setup

Experiments were carried out in real agriculture runoff from a farm land in Tehran, Iran. The runoff was further acidified to pH 2.8 with sulphuric acid and used within the next five days. The characteristics of runoff are shown in Table 1. A 2500 mL aqueous aliquot of the pesticide, at fixed pH, was placed in a The fiberglass-RPR with a maximum capacity of 7.5 L, a length of 50 cm, width of 15 cm and height 10 cm. It is separated by a central wall, forming two channels. The RPR includes a paddle wheel connected to an engine to obtain a mixed and homogeneous system. A halogen lamp (300 W, Osram, Munich, Germany, wavelength range: 400–800 nm) was placed upon the reactor (Fig. 1) and used as visible light source for the photocatalytic reactions that take place in solution exposed up to 1 h. The luminous intensity (lux) was measured using an illumination meter (LX-100S, KIMO, France) to estimate the light intensity, and was then converted to the irradiance unit (in W/m^2) using conversion factors (Thimijan and Heins, 1983). The light intensity of the light source was estimated to be 697 ± 5.33 lux (7.5 × 10–3 W/m^2), which is much lower than the global average solar irradiance (~10 W/m^2)(Mendoza et al., 2017).

2.3. Analytical determinations

Samples were taken at pre-selected time intervals and immediately centrifuged for 20 min at 6000 rpm. A Varian chrome pack CP–3800 gas chromatography was used to analyze CPF samples. The instrument was equipped with 63Ni electron capture detector (ECD) and a 30 m × 0.32 mm i.d. (0.25 μm film thickness) HP 5 ms fused silica capillary

Table 1
Characterization of agriculture runoff.

Parameters	Agriculture runoff
pH	6.8 ± 0.3
Conductivity (μS cm^{-1})	420 ± 0.8
Salinity (mg L^{-1})	0.22 ± 0.02
Total Dissolved Solid (TDS) (mg L^{-1})	210 ± 0.94
Total Nitrogen (mg L^{-1})	1.8 ± 0.16
Total Phosphorous (mg L^{-1})	0.34 ± 01

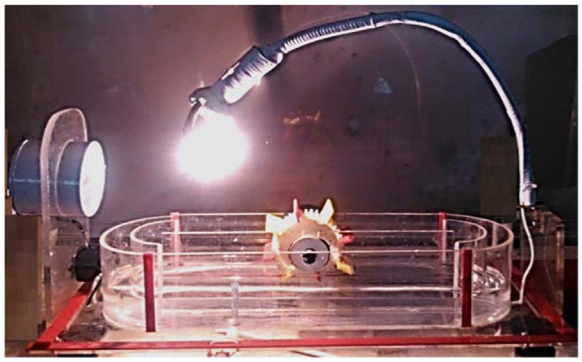

Fig. 1. The raceway pond reactor (RPR) used in the experiments.

Table 2
Independent variables and levels (coded and uncoded) of central composite design.

TiO_2 solar photocatalysis						
Independent variables	Symbol			Levels of variables		
		-1	-0.59	0	+0.59	+1
Chlorpyrifos Concentration (ppm)	X1	1.0	1.6	2.5	3.4	4.0
Time (min)	X2	5.0	16.0	32.0	49.0	60.0
TiO_2 dosage (mg L^{-1})	X3	0.0	10.0	25.0	40.0	50.0

column. Nitrogen gas (99.999%) was used as a carrier gas at a flow rate of 1.5 mL/min. Oven temperature was kept at 90 °C for 1 min then increased to 170 °C at a rate of 3.5 °C/min, and finally to 280 °C at rate of 10 °C/min. The injector and the detector temperatures were adjusted to 250 °C and 300 °C respectively. 1 µl of each sample was injected to GC-ECD for separation and quantitative analysis. Total Nitrogen and Phosphorous were measured using Hach test kit (Germany).

2.4. Design of experiment using central composite design (CCD)

Half fractional factorial design was carried out to determine which experimental variables and their interactions present significant effects. Then, a central composite rotatable design for three independent variables was employed to design experiments. A five level, three variables central composite rotatable design was employed for optimization with respect to three important reaction variables: Chlorpyrifos concentration (X_1), Time (X_2) and TiO_2 dosage (X_3). Design generation and statistical analysis were performed using the R software by RSM package (Lenth, 2009; Yaghmaeian et al., 2016). The independent variables and their levels are shown in Table 2. According to the Montgomery method (Myers et al., 2016), the total number of experiments carried out was 23.

Table 4
Estimated regression coefficients for removal efficiency by TiO_2 solar photocatalysis.

Coefficients:					
	Estimate	**SE**	**t**	**P**	
(Intercept)	66.08502	0.85132	77.6262	< 2.2e−16	***
X1	−3.35676	1.15668	−2.9021	0.01095	*
X2	31.32044	1.15663	27.0791	3.765e−14	***
X3	−6.10386	1.15683	−5.2764	9.314e−05	***
X2:X3	−20.56546	2.50895	−8.1968	6.375e−07	***
X1^2	10.27664	1.80618	5.6897	4.289e−05	***
X2^2	−17.86612	1.80721	−9.8860	5.809e−08	***
X3^2	−38.44836	1.80618	−21.2872	1.276e−12	***

Signif. codes: 0 '***' 0.001 '**' 0.01 '*' 0.05 '.' 0.1 ' ' 1. where: SE = standard error, t = student test, p = probability.

Table 5
Analysis of variance (ANOVA) for the fitted polynomial model for CPF removal using TiO_2 solar photocatalysis.

Model formula	Df	Sum Sq	Mean Sq	F value	Pr(> F)
First-order response	3	4936.7	1645.56	252.0400	4.724e−13
Two way interaction	1	438.7	438.67	67.1880	6.375e−07
Pure quadratic response	3	3807.9	1269.32	194.4132	3.163e−12
Residuals	15	97.9	6.53	–	–
Lack of fit	7	36.2	5.18	0.6714	0.6936
Pure error	8	61.7	7.71	–	–

Note: Multiple R^2: 0.9894, Adjusted R^2: 0.9845, F-statistic: 200.9 on 7 and 15 DF, p-value: 1.137e−13.

Table 3
Independent variables and results for CPF degradation by Central Composite Design (CCD).

Run order	Coded variables			Actual variables			Response	
	X1	X2	X3	CPF	Time	TiO_2	Experimental (%)	Predicted (%)
1	0.00	0.00	0.00	2.50	32.00	25.00	64.24	66.08
2	0.00	0.00	0.00	2.50	32.00	25.00	64.80	66.08
3	0.00	0.00	0.00	2.50	32.00	25.00	65.20	66.08
4	−0.59	0.59	−0.59	1.60	49.00	10.00	82.20	81.28
5	0.59	0.59	−0.59	3.40	49.00	10.00	75.67	77.32
6	0.00	0.00	0.00	2.50	32.00	25.00	65.60	66.08
7	−0.59	−0.59	0.59	1.60	16.00	40.00	37.25	37.12
8	0.00	0.00	0.00	2.50	32.00	25.00	63.60	66.08
9	0.00	0.00	0.00	2.50	32.00	25.00	62.04	66.08
10	0.00	0.00	0.00	2.50	32.00	25.00	64.80	66.08
11	0.59	0.59	0.59	3.40	49.00	40.00	55.50	55.79
12	−0.59	0.59	0.59	1.60	49.00	40.00	57.25	59.76
13	−0.59	−0.59	−0.59	1.60	16.00	10.00	30.37	30.00
14	0.59	−0.59	0.59	3.40	16.00	40.00	34.35	33.16
15	0.59	−0.59	−0.59	3.40	16.00	10.00	27.17	26.04
16	0.00	0.00	0.00	2.50	32.00	25.00	68.00	66.08
17	0.00	0.00	1.00	2.50	32.00	50.00	21.20	21.53
18	0.00	−1.00	0.00	2.50	5.00	25.00	13.60	16.89
19	0.00	0.00	−1.00	2.50	32.00	0.00	31.60	33.74
20	1.00	0.00	0.00	4.00	32.00	25.00	71.25	73.01
21	0.00	0.00	0.00	2.50	32.00	25.00	71.60	66.08
22	−1.00	0.00	0.00	1.00	32.00	25.00	79.00	79.72
23	0.00	1.00	0.00	2.50	60.00	25.00	81.52	79.54

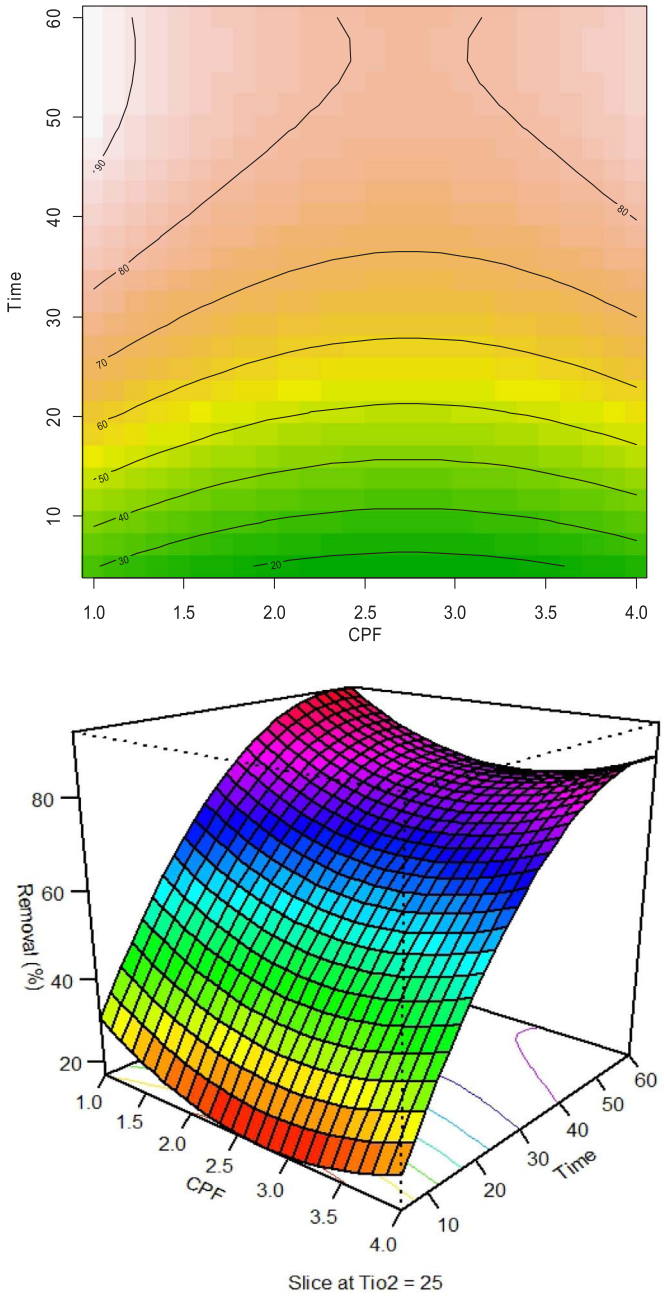

Fig. 2. Contour (above) and 3D response surface (below) plots of CPF removal (%) at pH = 6.8 ± 0.3 as a function of CFC concentration (mg L^{-1}) and time (min).

The data from the design were used to create a prediction model. The empirical second order polynomial model was shown as follows (Eq. (9)):

$$Y = \beta_0 + \sum_{j=1}^{K} \beta_j x_j + \sum_{j=1}^{K} \beta_{jj} x_j^2 + \sum \sum_{i<j=2}^{K} \beta_{ij} x_i x_j \quad (9)$$

where Y is the response; x_i and x_j are variables (i and j ranged from 1 to k); β_0 is the constant term; β_j is the linear coefficient, β_{ij} is the interaction coefficient, and β_{jj} is the quadratic coefficient; k is the number of independent parameters ($k = 3$ in this study) (Zhang et al., 2014).

2.5. Statistical analysis

The experimental data were analyzed by multiple regression analysis through the generalized least square to find out the relationship between the independent and dependent variables using R software (3.0.3). Also, stationary point in original units, as a result of analysis of variance Table in R software, was used to estimate an optimal condition for CPF removal.

3. Result and discussion

3.1. Model fitting and statistical analysis

A second-order model can be constructed efficiently with CCD (Myers et al., 2016). CCD is first-order (2 N) designs augmented by additional center and axial points to allow estimation of the tuning parameters of a second-order model. According to the created design, 23 experiments were performed for TiO_2 solar photocatalysis treatment processes. Table 3 shows the Independent variables, experimental and predicted results for CPF degradation by Central Composite Design (CCD). Various models were tested and a quadratic model was selected as the best for percentage oxidation of CPF. According to Table 4, the coefficient of the model for the response was estimated using multiple regression analysis technique included in the RSM. The quadratic model thus obtained was given as follows by Eq. (10):

$$\begin{aligned} \mathbf{Y\ (CPF\ Removal}\ (\%)) = {} & 66.08502 - 3.35676{*}X1 + 31.32044{*}X2 \\ & - 6.103869{*}X3 - 20.56546{*}X2{*}X3 + 10.27664{*}X1^2 \\ & - 17.86612{*}X2^2 - 38.44836{*}X3^2 \end{aligned} \quad (10)$$

The fit of the model was verified by the coefficient of determination R^2 and p-value for lack of fit. As shown in Table 5 the R^2 value was 0.989 which indicated that about 1.1% of the total variations were not satisfactorily explained by the predicted model. The R^2-adj value of 0.984 indicated the high degree of correlation between the observed and predicted values for the CPF removal efficiency in the model. The fact that R^2 is large does not mean that the model is the best. For this reason, the variance was used to measure the lack of fit between the model and the experimental data: this was the sum of the squares of the difference between the response variable and the fitted values predicted by the model. Tables 3 and 5 show that there is no significant difference between observed and predicted model data (p-value of lack of fit > 0.05), so the model indicates a good model prediction for CPF removal. A very high F-value (F-statistic = 200.9, much greater than unity) and a very low probability value (p-value = 1.137e-13) indicate that the models obtained was highly significant.

It could be seen from Table 4 that the linear coefficients (X1, X2, X3), a quadratic term coefficient (X1^2, X2^2, X3^2) and cross product coefficients (X2:X3) were significant, with very small P-values ($P < 0.01$). The other term coefficients were not significant ($P > 0.05$) that were removed from the model. Therefore, X1, X3, X2, X1^2, X2^2, X3^2 and X2:X3 were important factors in the oxidation process of CPF.

3.2. Effect of CPF concentration in different time periods

The main interest of this study is to investigate the degradation of CPF in real conditions at pilot plant scale. The degradation of CPF was visualized through both contour plot and three-dimensional (3D) view of response surface graphs (Fig. 2). The graphs were plotted as a function of two factors CPF and Time at a time, keeping TiO_2 at a fixed level (25 mg L^{-1}). As shown, the efficiency of CPF degradation was increased by increasing its concentration and time in the TiO_2 solar photocatalysis. This is attributed to the need for more reactive species ($^{\bullet}OH$ and $^{\bullet}O_2^-$) for the oxidation of higher pollutant loads since the formation of these reactive species on the catalyst surface. This means that RPR designed has a good efficiency in degradation of high CPF concentration. Therefore, the available $^{\bullet}O_2^-$ radicals were suitable for the degradation of the pollutants at higher concentrations as a result of favorable aeration (Bahnemann et al., 2007; Hoseini et al., 2013a). It also appears that, under favorable aeration conditions, superoxide anion radicals were produced through the scavenging effect of

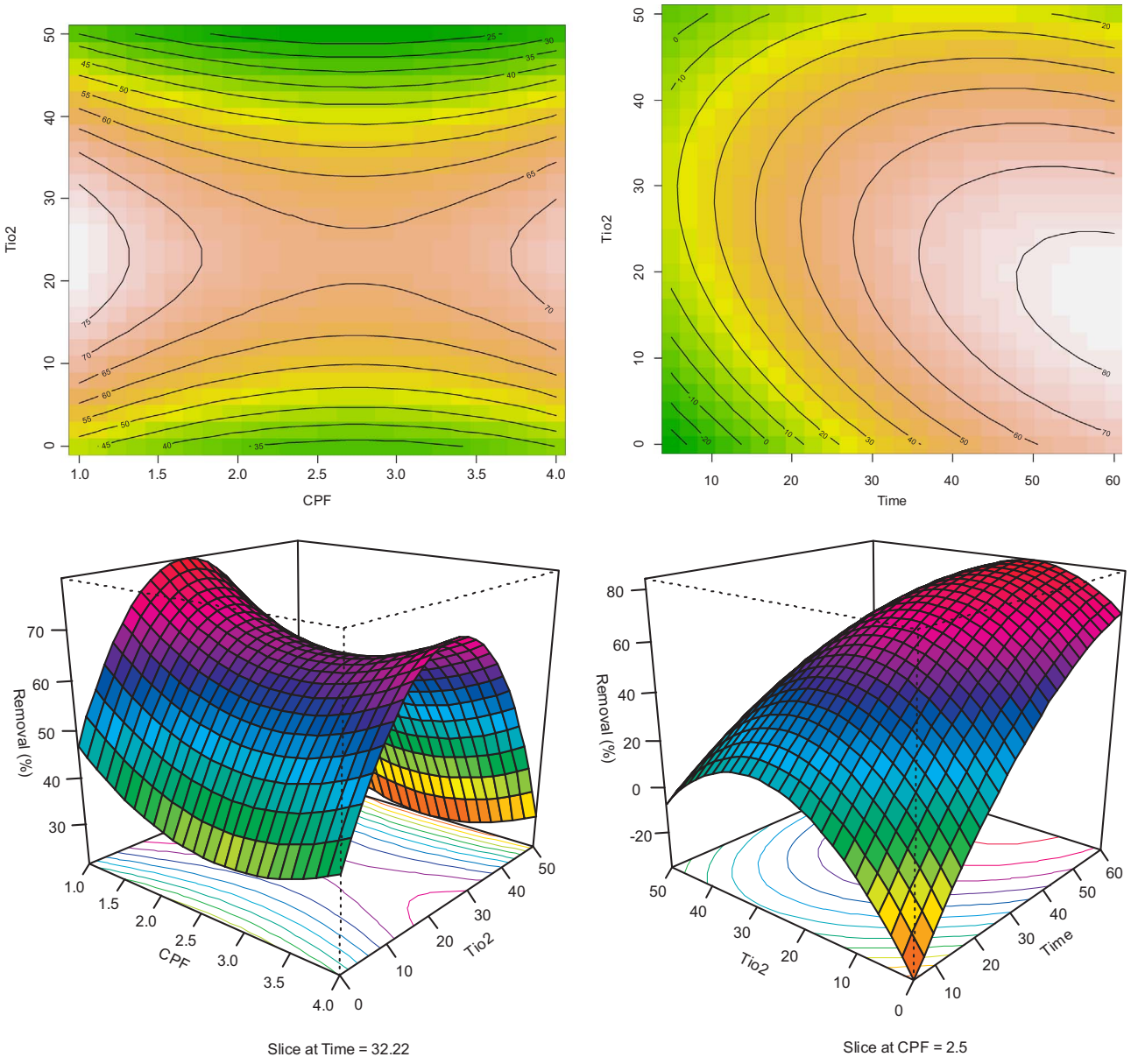

Fig. 3. Contour (above) and 3D response surface (below) plots of CPF removal (%) at pH = 6.8 ± 0.3 as a function of (a) CFC concentration (mg L^{-1}) and catalyst dosage (mg L^{-1}), and (b) time (min) and catalyst dosage (mg L^{-1}).

conduction band electrons by the dissolved O_2 molecules. In addition, as oxygen increases, the rate of ROS production increases due to the decrease in the rate of recombination that takes place (Fagan et al., 2016). The water matrix used in the experiments contained 1.6 mg L^{-1} and 0.35 mg L^{-1} of Total Nitrogen and Total Phosphorous respectively with Conductivity 420 (μS cm^{-1}). Therefore, it was expected that some of the hydroxyl radicals generated during the treatment would react with organic molecules other than the target compounds. As a consequence, the presence of all these species and compounds in the runoff must be taken into account as they usually decrease the rate of reaction compared to water containing less organic matter and inorganic components (Carra et al., 2015).

Table 6
Predicted and coded experimental values of the responses at optimum conditions.

Optimum condition			CPF removal (%)	
CPF (X1)	Time (X2)	TiO_2 (X3)	Experimental[a]	Predicted
0.163	1.089	−0.37	80 ± 1.42	84.01

[a] Mean ± standard deviation (n = 3).

3.3. Effect of TiO_2 dosage in different time periods

The effect of catalyst dose on the degradation efficiency of CPF was studied by varying dose from 0 to 50 mg L^{-1} of TiO_2. It was observed that, the percentage of degradation improved with increasing catalyst and time, till a decrease was observed more than 40 mg L^{-1} of TiO_2, as shown in Fig. 3.

The 3D response surface and the 2D contour plots in Fig. 3 show the relationship between CPF removal as response and experimental levels of variables (CPF, Time, TiO_2) and the type of their interactions. Response surface plots show that at low and high levels of the TiO_2 the oxidation of CPF was minimal. In fact, there was a region in which

neither a rising trend nor a decreasing trend in the oxidation was observed. This phenomenon confirms that there was an existence of optimum for the TiO_2 dosage to maximize the oxidation process. By increasing the dose of TiO_2, the amount of UV light photons and the number of CPF molecules absorbed on the surface of the catalyst was increased, which leads to an increase in the rate of photocatalytic reaction. However, above certain dose agglomeration (particle-particle interaction) of catalyst takes place, and thus, causes a decrease in the number of active sites on its free surface and, therefore, a drop in the photocatalytic degradation rate. Thus, the decrease in degradation was due to the decrease in surface area of catalyst related to the aggregation of TiO_2. The increased turbidity of the suspension by the higher dose of photocatalyst, which causes a decrease in the penetration of UV rays, dispersion of visible light and screening effects, and hence photo activated volume of suspension decreases can be considered as another reason (Adesina, 2004; Hoseini et al., 2013a; Malato et al., 2000). Also by increasing the time, CPF concentration has decreased due to the creation of more reactive species.

The shapes of the contour plots, circular or elliptical, indicated significant or no significant of interactions between the variables. Circular contour plot indicated that the interactions between the corresponding variables could be negligible, while elliptical contour plot indicates that the interactions could be significant (Shao et al., 2011). As illustrated in Table 4 and Fig. 3, the curved contour lines showed that there was an interaction between time and TiO_2 which was reflected by the corresponding P value ($P < 0.001$) in Table 4.

3.4. Validation of the model

The optimum oxidation conditions {X1 = [2.74 ppm (0.163)], X2 = [62.5 min (1.089)] and X3 = [15.72 mg L^{-1} (−0.37)]} for the CPF removal were suggested by Analysis of Variance Table of R software. The theoretical CPF removal that was predicted under the above conditions was 84.01%. This set of conditions was determined to be optimum by the RSM optimization approach and was also used to validate experimentally and predict the values of the responses using the model equation. The mean removal efficiency for CPF was 80 ± 1.42 (n = 3), corresponding well to the predicted value of the model equation, which confirmed that the response model was adequate for the optimization (Table 6).

4. Conclusions

The results presented show the efficiency and feasibility of using RPR at low concentration of TiO_2 for the elimination of CPF with the treatment processes of TiO_2 solar photocatalysis. RPR involves simple design and materials and would significantly reduce depreciation costs compared with CPCs for this application. ANOVA was applied to achieve the prediction model. According to the stationary point in original units, the optimum condition for the removal of 84.01% CPF was obtained as follow: CPF [2.74 ppm (0.163)], Time [62.5 min (1.089)] and dosage of TiO_2 [15.72 mg L^{-1} (−0.37)]. These facts encourage the use of RPR on a commercial scale as tertiary treatment and further research on process optimization is needed to allow for a more detailed economic evaluation.

Acknowledgments

The authors wish to extend special recognition to the Tehran University of Medical Sciences for the financial support to carry out this project (No. 95-01-46-31412).

References

Adesina, A., 2004. Industrial exploitation of photocatalysis: progress, perspectives and prospects. Catal. Surv. Asia 8, 265–273.
Affam, A.C., Chaudhuri, M., 2013. Degradation of pesticides chlorpyrifos, cypermethrin and chlorothalonil in aqueous solution by TiO2 photocatalysis. J. Environ. Manag. 130, 160–165.
Ahmed, S., Rasul, M., Brown, R., Hashib, M., 2011. Influence of parameters on the heterogeneous photocatalytic degradation of pesticides and phenolic contaminants in wastewater: a short review. J. Environ. Manag. 92, 311–330.
Amalraj, A., Pius, A., 2015. Photocatalytic degradation of monocrotophos and Chlorpyrifos in aqueous solution using TiO_2 under UV radiation. J. Water Process Eng. 7, 94–101.
Bahnemann, W., Muneer, M., Haque, M.M., 2007. Titanium dioxide-mediated photocatalysed degradation of few selected organic pollutants in aqueous suspensions. Catal. Today 124, 133–148.
Bezerra, M.A., Santelli, R.E., Oliveira, E.P., Villar, L.S., Escaleira, L.Al, 2008. Response surface methodology (RSM) as a tool for optimization in analytical chemistry. Talanta 76, 965–977.
Carra, I., Santos-Juanes, L., Acién Fernández, F.G., Malato, S., Sánchez Pérez, J.A., 2014. New approach to solar photo-Fenton operation. Raceway ponds as tertiary treatment technology. J. Hazard. Mater. 279, 322–329.
Carra, I., Sirtori, C., Ponce-Robles, L., Sánchez Pérez, J.A., Malato, S., Agüera, A., 2015. Degradation and monitoring of acetamiprid, thiabendazole and their transformation products in an agro-food industry effluent during solar photo-Fenton treatment in a raceway pond reactor. Chemosphere 130, 73–81.
Choi, W., Termin, A., Hoffmann, M.R., 1994. The role of metal ion dopants in quantum-sized TiO_2: correlation between photoreactivity and charge carrier recombination dynamics. J. Phys. Chem. 98, 13669–13679.
Dehghani, M.H., Faraji, M., Mohammadi, A., Kamani, H., 2017. Optimization of fluoride adsorption onto natural and modified pumice using response surface methodology: isotherm, kinetic and thermodynamic studies. Korean J. Chem. Eng. 34, 454–462.
Ejaz, M., Afzal, M.B.S., Shabbir, G., Serrão, J.E., Shad, S.A., Muhammad, W., 2017. Laboratory selection of Chlorpyrifos resistance in an Invasive Pest, Phenacoccus solenopsis (Homoptera: pseudococcidae): Cross-resistance, stability and fitness cost. Pestic. Biochem. Physiol. 137, 8–14.
EPA, 2015. Revised Human Health Risk Assessment on Chlorpyrifos. URL: ⟨https://www.epa.gov/ingredients-used-pesticide-products/revised-human-health-risk-assessment-Chlorpyrifos⟩.
Fagan, R., McCormack, D.E., Dionysiou, D.D., Pillai, S.C., 2016. A review of solar and visible light active TiO_2 photocatalysis for treating bacteria, cyanotoxins and contaminants of emerging concern. Mater. Sci. Semicond. Process. 42, 2–14.
Fujishima, A., Rao, T.N., Tryk, D.A., 2000. Titanium dioxide photocatalysis. J. Photochem. Photobiol. C: Photochem. Rev. 1, 1–21.
Fujishima, A., Zhang, X., 2006. Titanium dioxide photocatalysis: present situation and future approaches. C. R. Chim. 9, 750–760.
Gaya, U.I., Abdullah, A.H., 2008. Heterogeneous photocatalytic degradation of organic contaminants over titanium dioxide: a review of fundamentals, progress and problems. J. Photochem. Photobiol. C: Photochem. Rev. 9, 1–12.
Hoffmann, M.R., Martin, S.T., Choi, W., Bahnemann, D.W., 1995. Environmental applications of semiconductor photocatalysis. Chem. Rev. 95, 69–96.
Hoseini, M., Nabizadeh, R., Nazmara, S., Safari, G.H., 2013a. Influence of under pressure dissolved oxygen on trichloroethylene degradation by the H_2O_2/TiO_2 process. J. Environ. Health Sci. Eng. 11, 38.
Hoseini, M., Safari, G.H., Kamani, H., Jaafari, J., Ghanbarain, M., Mahvi, A.H., 2013b. Sonocatalytic degradation of tetracycline antibiotic in aqueous solution by sonocatalysis. Toxicol. Environ. Chem. 95, 1680–1689.
Ismail, M., Khan, H.M., Sayed, M., Cooper, W.J., 2013. Advanced oxidation for the treatment of Chlorpyrifos in aqueous solution. Chemosphere 93, 645–651.
Khan, R., Kim, S.W., Kim, T.-J., Nam, C.-M., 2008. Comparative study of the photocatalytic performance of boron–iron Co-doped and boron-doped TiO_2 nanoparticles. Mater. Chem. Phys. 112, 167–172.
Lenth, R.V., 2009. Response-surface methods in R, using rsm. J. Stat. Softw. 32, 1–17.
Malato, S., Blanco, J., Maldonado, M., Fernández-Ibáñez, P., Campos, A., 2000. Optimising solar photocatalytic mineralisation of pesticides by adding inorganic oxidising species; application to the recycling of pesticide containers. Appl. Catal. B: Environ. 28, 163–174.
Mendoza, J.A., Lee, D.H., Kang, J.-H., 2017. Photocatalytic removal of gaseous nitrogen oxides using WO_3/TiO_2 particles under visible light irradiation: effect of surface modification. Chemosphere 182, 539–546.
Myers, R.H., Montgomery, D.C., Anderson-Cook, C.M., 2016. Response Surface Methodology: Process and Product Optimization Using Designed Experiments. John Wiley & Sons.
Saini, R., Kumar, P., 2016. Optimization of Chlorpyrifos degradation by Fenton oxidation using CCD and ANFIS computing technique. J. Environ. Chem. Eng. 4, 2952–2963.
Shao, Q., Deng, Y., shen, H., Fang, H., Zhao, X., 2011. Optimization of polysaccharides extraction from Tetrastigma hemsleyanum Diels et Gilg using response surface methodology. Int. J. Biol. Macromol. 49, 958–962.
Sharbidre, A.A., Metkari, V., Patode, P., 2011. Effect of methyl parathion and Chlorpyrifos on certain biomarkers in various tissues of guppy fish, Poecilia reticulata. Pestic. Biochem. Physiol. 101, 132–141.
Sivagami, K., Vikraman, B., Krishna, R.R., Swaminathan, T., 2016. Chlorpyrifos and endosulfan degradation studies in an annular slurry photo reactor. Ecotoxicol. Environ. Saf. 134 (Part 2), 327–331.
Thimijan, R.W., Heins, R.D., 1983. Photometric, radiometric, and quantum light units of measure: a review of procedures for interconversion. HortScience 18, 818–822.
UNEP, 2012. POPRC-8/6: Assessment of alternatives to endosulfan. International Institute for Sustainable Development (IISD), Geneva. URL: ⟨https://www.google.com/url?Sa = t&rct = j&q = &esrc = s&source = web&cd = 1&ved = 0ahUKEwimjrPmrMPVAhXMuxQKHTdQB54QFggnMAA&url = http%3A%2F%2Fchm.pops.int%2FPortals%2F0%2Fdownload.aspx%3Fd%3DUNEP-POPS-

POPRC.8-POPRC-8-6.English.pdf&usg = AFQjCNEs7Yh8F0KpCf2FO2h3ctMSqF9R3w〉.
Wang, C.-y., Pagel, R., Dohrmann, Jr.K., Bahnemann, D.W., 2006. Antenna mechanism and deaggregation concept: novel mechanistic principles for photocatalysis. C. R. Chim. 9, 761–773.
WHO, 2009. WHO specifications and evaluations for public health pesticides, Chlorpyrifos. URL: 〈www.who.int/whopes/quality/Chlorpyrifos_WHO_specs_eval_Mar_2009.pdf〉.
Yaghmaeian, K., Silva Martinez, S., Hoseini, M., Amiri, H., 2016. Optimization of As (III) removal in hard water by electrocoagulation using central composite design with response surface methodology. Desalin. Water Treat. 57, 27827–27833.
Zhang, X., Chen, J., Mao, M., Guo, H., Dai, Y., 2014. Extraction optimization of the polysaccharide from Adenophorae Radix by central composite design. Int. J. Biol. Macromol. 67, 318–322.
Zimbron, J.A., Reardon, K.F., 2009. Fenton's oxidation of pentachlorophenol. Water Res. 43, 1831–1840.